Published in final edited form as:
FEBS J. 2013 July ; 280(14): 3232–3243. doi:10.1111/febs.12305.

Insulin receptor substrate-2 is expressed in kidney epithelium and up-regulated in diabetic nephropathy

Michelle B. Hookham[1,*], **Helen C. O'Donovan**[2,*], **Rachel H. Church**[1], **Annie Mercier-Zuber**[3], **Lucilla Luzi**[4], **Simon P. Curran**[2], **Rosemarie M. Carew**[2], **Alejandra Droguett**[5], **Sergio Mezzano**[5], **Markus Schubert**[6], **Morris F. White**[7], **John K. Crean**[2], and **Derek P. Brazil**[1]

[1]Centre for Vision and Vascular Science, Queen's University Belfast, UK [2]University College Dublin Diabetes Research Centre, Conway Institute, University College Dublin, Ireland [3]Department of Medicine, University of Cambridge, UK [4]Department of Experimental Oncology, European Institute of Oncology, Milan, Italy [5]Department of Nephrology, School of Medicine, Universidad Austral, Valdivia, Chile [6]Department of Internal Medicine II, Centre for Molecular Medicine Cologne, University of Cologne, Germany [7]Howard Hughes Medical Institute, Division of Endocrinology, Children's Hospital Boston, MA, USA

Abstract

Diabetic nephropathy (DN) is a progressive fibrotic condition that may lead to end-stage renal disease and kidney failure. Transforming growth factor-β1 and bone morphogenetic protein-7 (BMP7) have been shown to induce DN-like changes in the kidney and protect the kidney from such changes, respectively. Recent data identified insulin action at the level of the nephron as a crucial factor in the development and progression of DN. Insulin requires a family of insulin receptor substrate (IRS) proteins for its physiological effects, and many reports have highlighted the role of insulin and IRS proteins in kidney physiology and disease. Here, we observed IRS2 expression predominantly in the developing and adult kidney epithelium in mouse and human. BMP7 treatment of human kidney proximal tubule epithelial cells (HK-2 cells) increases IRS2 transcription. In addition, BMP7 treatment of HK-2 cells induces an electrophoretic shift in IRS2 migration on SDS/PAGE, and increased association with phosphatidylinositol-3-kinase, probably due to increased tyrosine/serine phosphorylation. In a cohort of DN patients with a range of chronic kidney disease severity, IRS2 mRNA levels were elevated approximately ninefold, with the majority of IRS2 staining evident in the kidney tubules in DN patients. These data show that IRS2 is expressed in the kidney epithelium and may play a role in the downstream protective events triggered by BMP7 in the kidney. The specific up-regulation of IRS2 in the kidney tubules of DN patients also indicates a novel role for IRS2 as a marker and/or mediator of human DN progression.

Correspondence: D. P. Brazil, Centre for Vision and Vascular, Science, Queen's University Belfast, UK, Fax: +44 28 9063 2699, Tel: +44 28 9063 2572, d.brazil@qub.ac.uk, Website: http://Go.qub.ac.uk/dbrazil.
*These authors contributed equally to this work.

Supporting information
Additional supporting information may be found in the online version of this article at the publisher's web site:
Fig. S1. BMP7 drives IRS2 phosphorylation in HeLa cells.

Keywords

bone morphogenetic protein; diabetes; insulin receptor substrate; kidney; nephropathy

Introduction

Diabetes is a metabolic disorder characterized by a failure of insulin production by the pancreatic β-cells and insulin resistance at the level of muscle, liver and adipose [1]. Diabetes is characterized by vascular complications of the large blood vessels of the heart, brain and lower limbs, as well as the smaller vessels in the kidney and eye [1]. Diabetic kidney disease or nephropathy (DN) is the leading cause of end-stage renal failure worldwide [2,3], and diabetic retinopathy is the primary cause of blindness in working age populations [4]. Current treatments for DN delay but do not prevent progression of the disease. Recent research has highlighted the role of insulin signalling directly on kidney cells in renal damage in DN [5].

Insulin action in metabolic and other tissues requires insulin receptor tyrosine kinase phosphorylation of insulin receptor substrate (IRS) proteins to trigger key cellular effects such as glucose uptake, cell proliferation and longevity [6]. IRS proteins act as molecular scaffolds, providing over 20 phosphotyrosine residues in YMXM, YVNI or YIDL motifs located in their C-termini as docking sites for downstream effectors such as the p85/55/50 subunits of phosphatidylinositol-3-kinase, Grb2 and SHP2 [6]. This mechanism facilitates mediation of activation of Akt, extracellular signal-regulated kinase and mammalian target of rapamycin signalling by insulin (and other growth factors such as insulin-like growth factor-1 and brain-derived neurotrophic factor) in an IRS protein-dependent manner. IRS proteins are also rich in serine and threonine residues, and phosphorylation on many of these sites, such as Ser307, by kinases such as jun N-terminal kinase-1, protein kinase C isoforms and mammalian target of rapamycin appear to inhibit IRS protein function, promoting insulin resistance in cell culture models [7–11]. In contrast to the results of these cell-based experiments, a recent paper showed that Ser307 is a positive regulatory site that maintains insulin signalling during states of insulin resistance [12].

There are three main IRS proteins in humans: IRS1, 2 and 4 [6]. IRS1 and 2 are widely expressed in most tissues, whereas IRS4 expression is restricted to the hypothalamus/pituitary gland and thymus [6]. Although these proteins are similar in overall structure and sequence, there are distinct physiological roles for the individual IRS proteins *in vivo*. For example, mice lacking IRS1 display reduced body size and mild insulin resistance, whereas *Irs2*−/− mice are of normal size but are profoundly diabetic due to pancreatic β-cell failure and hepatic insulin resistance [13–16]. Studies have highlighted roles for IRS proteins in the kidney, with *Irs2*−/− mice displaying altered insulin-stimulated bicarbonate re-absorption [17] and also reduced kidney size and altered Akt → glycogen synthase kinase-3 beta signalling [18]. At the level of the glomerulus, insulin signalling in the podocyte is critical for normal kidney function, and mice lacking the insulin receptor in the glomerular podocytes develop albuminuria and glomerulosclerosis in the absence of hyperglycemia [5]. Mima *et al.* identified insulin signalling pathways via IRS1 and protein kinase C-β in both

mouse glomeruli and kidney tubules, but observed diabetes-induced defects in insulin signalling in the glomerular compartment only [19]. In a small study of 32 subjects, a Gly972→Arg polymorphism in IRS1 was associated with decreased renal function, potentially due to impaired insulin signalling [20]. These and other data suggest that insulin receptor engagement of IRS proteins is a crucial component of kidney physiology and diabetic nephropathy.

Apart from insulin, growth factors such as vascular endothelial growth factor (VEGF) are implicated in development of normal glomerular filtration barriers, as well as having a protective action on the vasculature in the diabetic kidney and eye [21]. Excessive VEGF expression causes a dramatic loss of glomerular barrier integrity, with associated decreases in renal function [22,23]. Many factors such as insulin and VEGF appear to mediate their protective effect in the diabetic kidney at the level of the podocyte [24–26]. Bone morphogenetic protein-7 (BMP7) has also been identified as a ‘protector’ of kidney function, and mediates kidney repair in DN and other renal fibrosis models [27–32]. BMP7 also plays a role in the developing kidney, whereby BMP7 produced from the podocytes is crucial for normal nephron development [33]. BMP7 engages canonical Smad1/5/8 signalling to mediate its cellular effects in podocytes and other kidney cells, as well as extracellular signal-regulated kinase signalling in colon cancer cells [34,35].

Here, we report IRS2 expression in the developing and adult kidney tubular epithelial compartment. We demonstrate a link between BMP7 and IRS2 promoter activation and signalling in kidney tubule epithelial cells. Finally, we show that levels of IRS2 mRNA are dramatically up-regulated in the kidney tubules of diabetic nephropathy patients. These data shed new light on the role of IRS2 in diabetic kidney disease, and identify a novel non-canonical signalling pathway for BMP7 in kidney tubule cells.

Results

Previous data from our laboratory showed that IRS2 mRNA was present in murine kidney at higher levels than in metabolic tissues such as liver [18]. In contrast, IRS1 mRNA levels were similar in mouse liver and kidney, but were modestly up-regulated in *Irs2*−/− kidney extracts (data not shown). IRS2 was also detected in early E14.5 mouse kidney cortex (http://www.eurexpress.org/ee/databases/assay.jsp?assayID=euxassay_014216&image=01), whereas IRS4 expression was detected predominantly in pituitary gland and thymus (http://www.eurexpress.org/ee/databases/assay.jsp?assayID=euxassay_011002&image=01) (Fig. 1A). IRS1 expression was not detected in mouse embryo at this early developmental stage (http://www.eurexpress.org/ee/) [36]. Adult human kidney tubules were moderately positive for IRS2, whereas glomerular cells were not stained. In contrast, both tubular and glomerular compartments show moderate staining for IRS1 (www.proteinatlas.com) [37,38]. These data suggest distinct patterns of IRS gene expression during mammalian development and in adult kidney, and demonstrate IRS2 expression in the E14.5 mouse kidney cortex.

Detection of IRS2 protein in mouse kidney extracts was difficult using available antibodies, and required immunoprecipitation to enrich for IRS2 [18]. Immunohistochemistry using available antibodies did not identify specific IRS2 staining in discrete mouse kidney regions

or cell types (data not shown). To identify whether IRS2 was expressed in distinct nephron segments, mouse kidneys were microdissected into discrete compartments such as glomeruli, proximal tubule, loop of Henle and the distal tubule [39]. Western blotting of protein extracted from these regions showed that IRS2 was expressed predominantly in the distal convoluted tubule and cortical collecting duct, with weaker staining present in the proximal convoluted tubule and cortical connecting tubule (Fig. 1B,C). Together with data showing IRS2 expression in human tubular epithelial cell lines [18], these data suggest that IRS2 is predominantly expressed in tubular epithelial cells in the kidney.

Deletion of IRS2 causes an approximate 20% reduction in kidney size and weight in mice, potentially due to reduced proximal tubule volume [18]. Podocyte-specific deletion of BMP7 also caused renal hypoplasia in mice due to reduced proximal tubule numbers [33]. We therefore explored whether BMP7 and IRS2 signalling were linked in kidney epithelial cells. Treatment of HK-2 cells with BMP7 induced an ~ 2.5-fold increase in IRS2 mRNA after 24 h (Fig. 2A). To further explore this effect, we examined whether specific regions of the IRS2 promoter were involved in this BMP7-mediated activation. HK-2 cells were transfected with four constructs encoding various portions of the human IRS2 promoter (Fig. 2B) [40]. Similar to the effect seen with endogenous IRS2 mRNA, modest activation of IRS2 mRNA induction was seen in BMP7-treated cells versus controls (Fig. 2C). These data suggest that BMP7-mediated regulation of IRS2 mRNA levels in kidney epithelial cells is modest and may involve proximal promoter elements.

Bioinformatic analysis identified a series of conserved Smad4 transcription factor sites in human, mouse and rat *Irs2* genomic sequences. Regions proximal to the transcription start site (+/− 1500 bp) in the *Irs2* gene contained conserved transcription factor modules with predicted Smad4 (GCTCagac) binding sites on both forward and reverse strands (Fig. 3). Interestingly, given our previous data showing that IRS2 may also regulate transforming growth factor β1 (TGFβ1) signalling [41], conserved Smad3 sites were also identified in human, mouse and rat *Irs2* (data not shown). These data support a module by which BMP7 signalling via the canonical Smad signalling pathway directly regulates *Irs2* transcription in HK-2 cells.

IRS proteins such as IRS2 are heavily phosphorylated on a series of serine and tyrosine residues in response to ligands such as insulin [42], tumour necrosis factor α [43] and brain-derived neurotrophic factor [44]. These phosphorylation events lead to retarded IRS protein migration on SDS/PAGE, and play a key role in IRS2-mediated signal transduction to downstream effectors. We therefore examined whether BMP7 triggered IRS2 phosphorylation in HK-2 cells. BMP7 did not greatly alter the overall protein levels of IRS2 in HK-2 cells, but did induce an upward mobility shift after 24 h exposure (Fig. 4A). This effect was also observed with increasing concentrations of BMP7, with 200 $ng \cdot mL^{-1}$ BMP7 inducing a similar upward shift in IRS2 as 10 $ng \cdot mL^{-1}$ TGFβ1 (Fig. 4B). Western blotting with phosphotyrosine antibody indicated that BMP7 caused increased tyrosine phosphorylation of IRS2 in HK-2 cells (Fig. 4C). This effect on IRS2 mobility was also seen when HeLa cells were treated with BMP7 (Fig. S1). Importantly, the strongest degree of BMP7-induced IRS2 tyrosine phosphorylation coincided with the peak of Smad1/5/8 phosphorylation in both HK-2 and HeLa cells (Fig. 4C). Treatment of HK-2 cells with

BMP7 also increased association of IRS2 with the p85 regulatory subunits of phosphatidylinositol-3-kinase, involving phosphotyrosine residues on IRS2 engaging SH2 domains of p85 (Fig. 4D). Levels of BMP7-stimulated IRS2 binding to p85/p55 were similar to those seen with insulin treatment of HK-2 cells (Fig. 4D). These data demonstrate for the first time that IRS2 signalling is increased by exposure of HK-2 cells to BMP7.

Previous studies had identified single nucleotide polymorphisms in IRS2 that did not segregate strongly with diabetes (e.g. [45]). To extend our analysis, changes in overall IRS2 mRNA levels in diabetic nephropathy were examined in a small cohort of DN patients with marked proteinuria, which reached the nephrotic range in five patients (total urinary protein excretion rate > 3.5 g/24 h, Table 1). Calculation of estimated glomerular filtration rate indicated that all patients had chronic kidney disease of stage 3 or worse, with one patient (DN6) having stage 5 chronic kidney disease (Table 1). The levels of IRS mRNA were low in control, non-diabetic kidney (Table 1). Increased IRS2 levels were evident in kidney biopsies from DN patients, with predominant staining in the kidney tubules (Fig. 5C,D and Table 1). An approximate 9.7-fold increase in IRS2 mRNA was detected in DN patients compared to controls, showing for the first time that increased IRS2 gene expression is a feature of diabetic kidney disease. No significant changes in IRS2 mRNA were detected in biopsies from patients with non-diabetic glomerular diseases such as focal segmental glomerulosclerosis or membranous nephropathy (Fig. 5), suggesting that hyperglycaemia is the primary driver of IRS2 mRNA up-regulation in human diabetic kidneys.

Discussion

Here we show that IRS2 is expressed in the kidney epithelium and is regulated by BMP7 at the transcriptional level via putative Smad4 transcription factor binding sites. IRS2 undergoes tyrosine phosphorylation in response to BMP7, and is up-regulated in tubular epithelial cells in patients with diabetic nephropathy (DN), identifying IRS2 as a potential novel marker of DN in humans. A summary of these data is shown in Fig. 5.

IRS2 mRNA was detected in the cortex of the developing metanephros in E14.5 mice (Fig. 1A). Other regions with moderate IRS2 staining at this time point included the skin, primitive thymus and dorsal root ganglion (http://www.eurexpress.org/ee/databases/assay.jsp?assayID=euxassay_014216). The pattern of expression of IRS4 in E14.5 mouse (strong staining in the thyroid and pituitary, moderate staining in the mid-brain and hypothalamus; Fig. 1A and data not shown) suggests that distinct roles for these IRS proteins exist in different cell types and tissues during development. Previous work identified differences in IRS2 and IRS4 expression in adult mouse liver and muscle, as well as B-cells and brain [16,46,47]. The different expression patterns of IRS2 and IRS4 in developing and adult mouse tissues may be explained by differential promoter activation in response to tissue-specific ligands and transcription factors.

Given our previous data showing IRS2 expression in human kidney epithelial cell lines, and the fact that homozygous deletion of *Irs2* causes reduced kidney size in mice [18], we further explored the identification of IRS2 mRNA in developing renal cortex in mice. Microdissection of kidney compartments confirmed that IRS2 protein expression was

detected predominantly in distal convoluted tubules and cortical collecting ducts, supporting a role for IRS2 in kidney epithelial function (Fig. 1B,C). Previous groups have identified IRS2 expression in both normal breast epithelium and breast carcinoma cells, as well as intestinal epithelium and Mustela vison lung Mv1Lu epithelial cells [48,49]. Specifically, IRS2 appears to positively regulate metastasis in the breast, in contrast to IRS1 [48]. IRS2 expression was also identified in isolated renal proximal tubules of mice and MCT proximal tubule cells [17,50]. Importantly, insulin-stimulated bicarbonate absorption was significantly attenuated in *Irs2*−/− mice, suggesting a major role for IRS2 in this process [17]. As IRS2 protein expression is also detected in the tubular epithelium of adult human kidney (data not shown), these data strongly support a role for IRS2 in human renal epithelial cell physiology.

BMP7 is a key regulator of bone and kidney formation during development [51,52]. Mice lacking BMP7 in the kidney podocyte develop small hypoplastic kidneys with a reduced numbers of kidney tubules [33]. This phenotype was similar to the reduced kidney size seen in *Irs2*−/− mice from day 5 in development [18]. We therefore hypothesized that an epistatic signalling pathway involving BMP7 and IRS2 may exist in the developing kidney. BMP7 induced a 2.5-fold increase in IRS2 mRNA in human kidney epithelial (HK-2) cells (Fig. 2A), and also increased the activity of transfected IRS2 promoter/luciferase constructs (Fig. 2B,C). These data suggest that BMP7-mediated up-regulation of IRS2 may involve promoter regions at least 1000 bp upstream of the *Irs2* transcription start site. Bioinformatic analysis identified a series of conserved Smad4 transcription factor modules in the *Irs2* proximal promoter of human, mouse and rat (Fig. 3).These data suggest that canonical pSmad1/5/8 → Smad4 signalling may be involved in BMP7-mediated regulation of *Irs2* transcription. IRS2, like other members of the IRS protein family, is phosphorylated on tyrosine residues in response to growth factors such as insulin and insulin-like growth factor-1. In addition, IRS2 proteins are heavily phosphorylated on serine residues under basal conditions and in response to ligands such as tumour necrosis factor α [6,11]. Treatment of HK-2 cells with increasing amounts of BMP7 increased the migration of IRS2 on SDS/PAGE at 1 h and this was maintained for up to 24 h (Fig. 4A,B). This effect was also seen in HeLa cells (Fig. S1). Importantly, a more rapid activation of Smad1/5/8 phosphorylation in response to BMP7 was evident in HK-2 cells compared to HeLa cells (Fig. 4C and Fig. S1). Increased binding of phosphatidylinositol-3-kinase regulatory subunits to IRS2 was detected after treatment with BMP7 (Fig. 4D), suggesting that increased tyrosine phosphorylation may explain the shift in IRS2 mobility (Fig. 4C). Due to the poor quality of available phosphoserine antibodies, we were unable to determine whether BMP7 induced an increase in IRS2 serine phosphorylation. Recent data from Zhang *et al.* showed that BMP7 treatment overcame the differentiation defect in brown adipocytes lacking IRS1 [53]. Our data extend the cross-talk between insulin and BMP7 to the kidney, and demonstrate that BMP7 can drive IRS2 expression and tyrosine phosphorylation. Changes in non-canonical p38 mitogen-activated protein kinase signalling pathways as a result of BMP7 deletion were also observed in BMP7-null podocytes [33]. In contrast, no changes in p38MAPK phosphorylation were observed in *Irs2*−/− kidney (data not shown), confirming that BMP7 engages multiple downstream pathways to produce its cellular effects.

Previous reports have analysed changes in the *Irs2* gene sequence in diabetes. IRS2 Gly1057→Asp and Leu647→Val polymorphisms were identified in type 2 diabetes patients, but these polymorphisms were not associated with disease incidence [45,54,55]. More recently, several novel variants in the *Irs2* gene were discovered in patients with severe insulin resistance, but did not segregate with insulin resistance [56]. A region of chromosome 13 (13q33.3) that spans the *Irs2* gene was recently shown to be associated with susceptibility to kidney disease in type 1 and 2 diabetes [57]. IRS2 mRNA was detected at low levels in control, non-diabetic biopsies (Fig. 5B). Levels were also low in biopsies from focal segmental glomerulosclerosis and membranous nephropathy patients (Fig. 5 and Table 1). Significantly higher levels of IRS2 mRNA staining were detected in biopsies of DN patients compared to non-diabetic controls, predominantly in the tubular epithelium (Fig. 5C,D versus Fig. 5A,B). Although the patient cohort was small in this study, all DN patients presented with chronic kidney disease stage 3 or greater, with the highest level of IRS2 staining present in the patient with the most severely compromised renal function (DN6, Table 1). These data suggest that up-regulation of IRS2 expression is a feature of diabetic kidney disease. In contrast, levels of BMP7 are decreased in DN [28,58], with reduced BMP7 contributing to podocyte loss via reduced Smad5 signalling [28]. Our data suggest that hyper-glycaemia may be the primary driver of both increased IRS2 levels and decreased BMP7 levels in the diabetic kidney. BMP7-stimulated IRS2 expression may only be relevant in the normoglycaemic environment. Other potential mechanisms involved in IRS2 mRNA up-regulation in the diabetic kidney may involve elevated levels of insulin, insulin-like growth factor-1 or profibrotic factors such as angiotensin II and TGFβ1. Recent data from our laboratory have shown that TGFβ1 engages IRS2 in kidney epithelial cells, and that siRNA-mediated knockdown of IRS2 alters epithelial cell expression of E-cadherin [41]. Up-regulation of IRS2 levels in the diabetic kidney may form part of a protective mechanism to enhance insulin-mediated cell survival, or to limit the glucose-induced damage to tubular epithelial cell function. Further experiments are required to fully elucidate the role of IRS2 in the pathogenesis of diabetic kidney disease. Our data also suggest that IRS2 may serve as a novel biomarker for DN. Future studies involving larger numbers of patients with earlier stages of mild/moderate DN as well as other fibrotic disorders of the kidney will test this hypothesis.

Experimental procedures

Cell culture and stimulation

Human kidney proximal tubule (HK-2) cells were maintained in Dulbecco's modified Eagle's medium/Hams F12 medium containing L-glutamine (10 mM), penicillin/streptomycin (5 mg·mL^{-1}), insulin/transferrin sodium selenite liquid media supplement (1 x), epidermal growth factor (10 ng·mL^{-1}), hydrocortisone (36 ng·mL^{-1}) and tridothyronine (3 pg·mL^{-1}). HeLa cells were cultured in Dulbecco's modified Eagle's medium supplemented with 10% v/v fetal bovine serum and 100 μg·mL^{-1} primosin (Sigma-Aldrich, Dorset, UK). For BMP7 stimulations, cells were starved in serum-free RPMI medium for 24 h prior to stimulation with BMP7 (100–200 ng·mL^{-1}).

Protein extraction, quantification and preparation

Cells were washed with chilled 1× NaCl/P_i and lysed with the appropriate volume of working RIPA lysis buffer [17]. The Bradford assay was used to calculate protein concentration, and samples were separated by SDS/PAGE as previously described [18].

Immunoprecipitation

Whole-cell lysates (250 μg) in supplemented lysis buffer (25 mM Tris/Cl pH 7.4, 150 mM NaCl, 1 mM EDTA, 1% Nonidet P-40 and 5% glycerol) were pre-cleared with 20 μL Protein A/G–agarose beads, and 5 μL of polyclonal IRS2 primary antibody were added overnight at 4 °C with rotation. Then 20 μL Protein A/G–agarose beads were added for 1 h at 4 °C, and immunoprecipitates were collected by centrifugation at 3000 g for 5 min at 4°C. The beads were washed 3 times in lysis buffer plus Na_3VO_4, at 4°C resuspended in Western loading buffer, boiled and loaded on SDS/PAGE as previously described [18]. Densitometry was performed using IMAGEJ (http://rsbweb.nih.gov/ij/), and IRS2 band intensities were expressed as a ratio of β-actin loading control intensity for each sample.

IRS2 expression in embryo and adult kidney

Images of IRS2 and IRS4 *in situ* hybridization in mouse embryos at E14.5 were obtained from the EURExpress Transcriptome Database for Mouse Embryo (www.eurexpress.org/ee/) [36]. The images shown are section 17 for IRS2 and section 15 for IRS4, and are published with permission from Richard Baldock (MRC Human Genetics Unit, Edinburgh, UK). Images of IRS2 immunohistochemistry staining in adult kidney were obtained from the Swedish Human Protein Atlas project (www.proteinatlas.org) [37,38].

Real-time quantitative PCR

RNA was extracted from HK-2 cells using an RNeasy RNA extraction kit (Qiagen). Total DNaseI-treated RNA (2 μg) was reverse transcribed, and TaqMan PCR was performed using the human IRS2 real-time probe set (Hs00275843_s1, Applied Biosystems). The generated product was analyzed using an ABI Prism 7700 sequence detection system (Life Technologies, Paisley, UK). Data were analysed using the $\Delta\Delta C_t$ method and normalized to 18S levels.

Luciferase assay

HK-2 cells were seeded at 3.5×10^4 cells/well of a 24-well tissue culture plate, and 24 h later were transiently co-transfected with 0.1 μg of Renilla plasmid as an internal transfection control and 0.4 μg of the IRS2 promoter reporter constructs. Cells were treated with BMP7 (200 ng·mL^{-1}) for a further 24 h. IRS2 promoter activity was measured using a dual luciferase kit (Promega). Results were analyzed for statistical significance using one-way ANOVA.

Microdissection of nephron segments

Microdissection of kidneys from wild-type mice ($n = 4$) was performed at ~ 3 months of age as described previously [39]. The various parts of the nephron were microdissected under the microscope in ice-cold Dulbecco's modified Eagle's medium/Ham's F12 medium (1 : 1;

Life Technologies). Pools of 10–20 microdissected tubules in 5 μL Dulbecco's modified Eagle's medium/Ham's F12 medium (1 : 1) were then transferred to 5 μL of 2× protein sample buffer (123mM Tris/Cl pH6.8, 1% (w/v) SDS, 20% (v/v) glycerol, 1% β-mercaptoethanol 0.1% bromophenol blue). Extracts were separated by SDS/PAGE and probed via Western blotting as described.

In situ hybridization

Kidney samples were obtained by percutaneous renal biopsy from patients undergoing diagnostic evaluation at the Division of Nephrology, Austral University, Valdivia, Chile. The samples were studied with local hospital ethics committee approval after obtaining patient consent. Control human kidney specimens were taken from normal portions of renal tissue from patients who underwent surgery because of localized renal tumors.

In situ hybridization was performed using biotin-labelled human antisense IRS2 probes. Detection was performed by incubation with an avidin/alkaline phosphatase conjugate (Dako, Ely, Cambridgeshire, UK) for 30 min at room temperature, followed by washing for 5 min with 1× TBS. Reactivity was visualized using nitroblue tetrazolium and 5-bromo-4-chloro-indolylphosphate *p*-toluidine salt as the enzyme substrate. Signal quantification was performed by image analysis using a KZ 300 imaging system 3.0 (Zeiss, Munich, Germany).

Statistical analysis

Experiments were performed three times in duplicate except where otherwise stated. All data are presented as means ± SEM. For cell culture experiments, statistical significance was determined using Student's unpaired *t* test or one-way ANOVA with Dunnett's *post hoc* multiple comparison test. For IRS2 staining in human biopsies, data were analysed using the Mann–Whitney non-parametric *t* test to determine statistical significance.

Supplementary Material

Refer to Web version on PubMed Central for supplementary material.

Acknowledgments

We thank Angela Valverde (Universidad Autonoma de Madrid), Richard Coward (Bristol Heart Institute) and Jordan Kreidberg (Children's Hospital Boston) for sharing unpublished data and helpful discussions. D.P.B. is supported by the Department for Employment and Learning Northern Ireland, Diabetes UK, the UK Biotechnology and Biological Sciences Research Council and Action Medical Research UK. J.K.C. is supported by Science Foundation Ireland. S.M. is supported by grant number 1120480 from Fondecyt (Chile). We thank colleagues at EURexpress.org/ee and Human Protein Atlas for permission to publish images in Fig. 1.

Abbreviations

BMP7	bone morphogenetic protein-7
DN	diabetic nephropathy
HK-2	human kidney proximal tubule epithelial cells
IRS	insulin receptor substrate

TGFβ1	transforming growth factor β1
VEGF	vascular endothelial growth factor

References

1. Doria A, Patti ME, Kahn CR. The emerging genetic architecture of type 2 diabetes. Cell Metab. 2008; 8:186–200. [PubMed: 18762020]
2. Brosius FC 3rd, Alpers CE, Bottinger EP, Breyer MD, Coffman TM, Gurley SB, Harris RC, Kakoki M, Kretzler M, Leiter EH, et al. Mouse models of diabetic nephropathy. J Am Soc Nephrol. 2009; 20:2503–2512. [PubMed: 19729434]
3. Navarro-Gonzalez JF, Mora-Fernandez C, Muros de Fuentes M, Garcia-Perez J. Inflammatory molecules and pathways in the pathogenesis of diabetic nephropathy. Nat Rev Nephrol. 2011; 7:327–340. [PubMed: 21537349]
4. Zong H, Ward M, Stitt AW. AGEs, RAGE, and diabetic retinopathy. Curr Diab Rep. 2011; 11:244–252. [PubMed: 21590515]
5. Welsh GI, Hale LJ, Eremina V, Jeansson M, Maezawa Y, Lennon R, Pons DA, Owen RJ, Satchell SC, Miles MJ, et al. Insulin signaling to the glomerular podocyte is critical for normal kidney function. Cell Metab. 2010; 12:329–340. [PubMed: 20889126]
6. Cheng Z, Tseng Y, White MF. Insulin signaling meets mitochondria in metabolism. Trends Endocrinol Metab. 2010; 21:589–598. [PubMed: 20638297]
7. Aguirre V, Uchida T, Yenush L, Davis R, White MF. The c-Jun NH_2-terminal kinase promotes insulin resistance during association with insulin receptor substrate-1 and phosphorylation of Ser^{307}. J Biol Chem. 2000; 275:9047–9054. [PubMed: 10722755]
8. Carlson CJ, White MF, Rondinone CM. Mammalian target of rapamycin regulates IRS-1 serine 307 phosphorylation. Biochem Biophys Res Commun. 2004; 316:533–539. [PubMed: 15020250]
9. Giraud J, Haas M, Feener EP, Copps KD, Dong X, Dunn SL, White MF. Phosphorylation of Irs1 at SER-522 inhibits insulin signaling. Mol Endocrinol. 2007; 21:2294–2302. [PubMed: 17579213]
10. Gual P, Gremeaux T, Gonzalez T, Le Marchand-Brustel Y, Tanti JF. MAP kinases and mTOR mediate insulin-induced phosphorylation of insulin receptor substrate-1 on serine residues 307, 612 and 632. Diabetologia. 2003; 46:1532–1542. [PubMed: 14579029]
11. Zick Y. Ser/Thr phosphorylation of IRS proteins: a molecular basis for insulin resistance. Sci STKE. 2005; 2005:pe4. [PubMed: 15671481]
12. Copps KD, Hancer NJ, Opare-Ado L, Qiu W, Walsh C, White MF. Irs1 serine 307 promotes insulin sensitivity in mice. Cell Metab. 2010; 11:84–92. [PubMed: 20074531]
13. Araki E, Lipes MA, Patti ME, Bruning JC, Haag B 3rd, Johnson RS, Kahn CR. Alternative pathway of insulin signalling in mice with targeted disruption of the IRS-1 gene. Nature. 1994; 372:186–190. [PubMed: 7526222]
14. Kubota N, Tobe K, Terauchi Y, Eto K, Yamauchi T, Suzuki R, Tsubamoto Y, Komeda K, Nakano R, Miki H, et al. Disruption of insulin receptor substrate 2 causes type 2 diabetes because of liver insulin resistance and lack of compensatory b-cell hyperplasia. Diabetes. 2000; 49:1880–1889. [PubMed: 11078455]
15. Tamemoto H, Kadowaki T, Tobe K, Yagi T, Sakura H, Hayakawa T, Terauchi Y, Ueki K, Kaburagi Y, Satoh S, et al. Insulin resistance and growth retardation in mice lacking insulin receptor substrate-1. Nature. 1994; 372:182–186. [PubMed: 7969452]
16. Withers DJ, Gutierrez JS, Towery H, Burks DJ, Ren JM, Previs S, Zhang Y, Bernal D, Pons S, Shulman GI, et al. Disruption of IRS2 causes type 2 diabetes in mice. Nature. 1998; 391:900–904. [PubMed: 9495343]
17. Zheng Y, Yamada H, Sakamoto K, Horita S, Kunimi M, Endo Y, Li Y, Tobe K, Terauchi Y, Kadowaki T, et al. Roles of insulin receptor substrates in insulin-induced stimulation of renal proximal bicarbonate absorption. J Am Soc Nephrol. 2005; 16:2288–2295. [PubMed: 15975995]

18. Carew RM, Sadagurski M, Goldschmeding R, Martin F, White MF, Brazil DP. Deletion of Irs2 causes reduced kidney size in mice: role for inhibition of GSK3β? BMC Dev Biol. 2010; 10:73. [PubMed: 20604929]
19. Mima A, Ohshiro Y, Kitada M, Matsumoto M, Geraldes P, Li C, Li Q, White GS, Cahill C, Rask-Madsen C, et al. Glomerular-specific protein kinase Cβ-induced insulin receptor substrate-1 dysfunction and insulin resistance in rat models of diabetes and obesity. Kidney Int. 2012; 79:883–896. [PubMed: 21228767]
20. Thameem F, Puppala S, Schneider J, Bhandari B, Arya R, Arar NH, Vasylyeva TL, Farook VS, Fowler S, Almasy L, et al. The Gly(972)Arg variant of human *IRS1* gene is associated with variation in glomerular filtration rate likely through impaired insulin receptor signaling. Diabetes. 2012; 61:2385–2393. [PubMed: 22617042]
21. Sivaskandarajah GA, Jeansson M, Maezawa Y, Eremina V, Baelde HJ, Quaggin SE. Vegfa protects the glomerular microvasculature in diabetes. Diabetes. 2012; 61:2958–2966. [PubMed: 23093658]
22. Veron D, Reidy KJ, Bertuccio C, Teichman J, Villegas G, Jimenez J, Shen W, Kopp JB, Thomas DB, Tufro A. Overexpression of VEGF-A in podocytes of adult mice causes glomerular disease. Kidney Int. 2010; 77:989–999. [PubMed: 20375978]
23. Veron D, Bertuccio CA, Marlier A, Reidy K, Garcia AM, Jimenez J, Velazquez H, Kashgarian M, Moeckel GW, Tufro A. Podocyte vascular endothelial growth factor ($Vegf_{164}$) overexpression causes severe nodular glomerulosclerosis in a mouse model of type 1 diabetes. Diabetologia. 2011; 54:1227–1241. [PubMed: 21318407]
24. Eremina V, Cui S, Gerber H, Ferrara N, Haigh J, Nagy A, Ema M, Rossant J, Jothy S, Miner JH, et al. Vascular endothelial growth factor A signaling in the podocyte–endothelial compartment is required for mesangial cell migration and survival. J Am Soc Nephrol. 2006; 17:724–735. [PubMed: 16436493]
25. Eremina V, Sood M, Haigh J, Nagy A, Lajoie G, Ferrara N, Gerber HP, Kikkawa Y, Miner JH, Quaggin SE. Glomerular-specific alterations of VEGF-A expression lead to distinct congenital and acquired renal diseases. J Clin Invest. 2003; 111:707–716. [PubMed: 12618525]
26. Sison K, Eremina V, Baelde H, Min W, Hirashima M, Fantus IG, Quaggin SE. Glomerular structure and function require paracrine, not autocrine, VEGF– VEGFR-2 signaling. J Am Soc Nephrol. 2011; 21:1691–1701. [PubMed: 20688931]
27. Manson SR, Niederhoff RA, Hruska KA, Austin PF. The BMP7–Smad1/5/8 pathway promotes kidney repair after obstruction induced renal injury. J Urol. 2011; 185:2523–2530. [PubMed: 21527199]
28. Mitu GM, Wang S, Hirschberg R. BMP7 is a podocyte survival factor and rescues podocytes from diabetic injury. Am J Physiol Renal Physiol. 2007; 293:F1641–F1648. [PubMed: 17804487]
29. Sugimoto H, Grahovac G, Zeisberg M, Kalluri R. Renal fibrosis and glomerulosclerosis in a new mouse model of diabetic nephropathy and its regression by bone morphogenic protein-7 and advanced glycation end product inhibitors. Diabetes. 2007; 56:1825–1833. [PubMed: 17456853]
30. Wang S, de Caestecker M, Kopp J, Mitu G, Lapage J, Hirschberg R. Renal bone morphogenetic protein-7 protects against diabetic nephropathy. J Am Soc Nephrol. 2006; 17:2504–2512. [PubMed: 16899516]
31. Zeisberg M, Bottiglio C, Kumar N, Maeshima Y, Strutz F, Muller GA, Kalluri R. Bone morphogenic protein-7 inhibits progression of chronic renal fibrosis associated with two genetic mouse models. Am J Physiol Renal Physiol. 2003; 285:F1060–F1067. [PubMed: 12915382]
32. Zeisberg M, Hanai J, Sugimoto H, Mammoto T, Charytan D, Strutz F, Kalluri R. BMP7 counteracts TGF-β1-induced epithelial-to-mesenchymal transition and reverses chronic renal injury. Nat Med. 2003; 9:964–968. [PubMed: 12808448]
33. Kazama I, Mahoney Z, Miner JH, Graf D, Economides AN, Kreidberg JA. Podocytederived BMP7 is critical for nephron development. J Am Soc Nephrol. 2008; 19:2181–2191. [PubMed: 18923055]
34. Grijelmo C, Rodrigue C, Svrcek M, Bruyneel E, Hendrix A, de Wever O, Gespach C. Proinvasive activity of BMP7 through SMAD4/src-independent and ERK/Rac/JNK-dependent signaling pathways in colon cancer cells. Cell Signal. 2007; 19:1722–1732. [PubMed: 17478078]

35. Leeuwis JW, Nguyen TQ, Chuva de Sousa Lopes SM, Lopes SM, van der Giezen DM, van der Ven K, Rouw PJ, Offerhaus GJ, Mummery CL, Goldschmeding R. Direct visualization of Smad1/5/8-mediated transcriptional activity identifies podocytes and collecting ducts as major targets of BMP signalling in healthy and diseased kidneys. J Pathol. 2011; 224:121–132. [PubMed: 21381028]
36. Diez-Roux G, Banfi S, Sultan M, Geffers L, Anand S, Rozado D, Magen A, Canidio E, Pagani M, Peluso I, et al. A high-resolution anatomical atlas of the transcriptome in the mouse embryo. PLoS Biol. 2011; 9:e1000582. [PubMed: 21267068]
37. Uhlen M, Bjorling E, Agaton C, Szigyarto CA, Amini B, Andersen E, Andersson AC, Angelidou P, Asplund A, Asplund C, et al. A human protein atlas for normal and cancer tissues based on antibody proteomics. Mol Cell Proteomics. 2005; 4:1920–1932. [PubMed: 16127175]
38. Uhlen M, Oksvold P, Fagerberg L, Lundberg E, Jonasson K, Forsberg M, Zwahlen M, Kampf C, Wester K, Hober S, et al. Towards a knowledge-based human protein atlas. Nat Biotechnol. 2010; 28:1248–1250. [PubMed: 21139605]
39. Rafiqi FH, Zuber AM, Glover M, Richardson C, Fleming S, Jovanovic S, Jovanovic A, O'Shaughnessy KM, Alessi DR. Role of the WNK-activated SPAK kinase in regulating blood pressure. EMBO Mol Med. 2010; 2:63–75. [PubMed: 20091762]
40. Udelhoven M, Leeser U, Freude S, Hettich MM, Laudes M, Schnitker J, Krone W, Schubert M. Identification of a region in the human IRS2 promoter essential for stress induced transcription depending on SP1, NFI binding and ERK activation in HepG2 cells. J Mol Endocrinol. 2011; 44:99–113. [PubMed: 19755487]
41. Carew RM, Browne MB, Hickey FB, Brazil DP. IRS2 and FoxO3a signalling are involved in E-cadherin expression and TGF-β1-induced repression in kidney epithelial cells. FEBS J. 2011; 278:3370–3380. [PubMed: 21777391]
42. Sun XJ, Rothenberg P, Kahn CR, Backer JM, Araki E, Wilden PA, Cahill DA, Goldstein BJ, White MF. Structure of the insulin receptor substrate IRS-1 defines a unique signal transduction protein. Nature. 1991; 352:73–77. [PubMed: 1648180]
43. Rui L, Aguirre V, Kim JK, Shulman GI, Lee A, Corbould A, Dunaif A, White MF. Insulin/IGF-1 and TNF-α stimulate phosphorylation of IRS-1 at inhibitory Ser307 via distinct pathways. J Clin Invest. 2001; 107:181–189. [PubMed: 11160134]
44. Soiampornkul R, Tong L, Thangnipon W, Balazs R, Cotman CW. Interleukin-1β interferes with signal transduction induced by neurotrophin-3 in cortical neurons. Brain Res. 2008; 1188:189–197. [PubMed: 18036576]
45. D'Alfonso R, Marini MA, Frittitta L, Sorge R, Frontoni S, Porzio O, Mariani LM, Lauro D, Gambardella S, Trischitta V, et al. Polymorphisms of the insulin receptor substrate-2 in patients with type 2 diabetes. J Clin Endocrinol Metab. 2003; 88:317–322. [PubMed: 12519871]
46. Fantin VR, Lavan BE, Wang Q, Jenkins NA, Gilbert DJ, Copeland NG, Keller SR, Lienhard GE. Cloning, tissue expression, and chromosomal location of the mouse insulin receptor substrate 4 gene. Endocrinology. 1999; 140:1329–1337. [PubMed: 10067860]
47. Sun XJ, Pons S, Wang LM, Zhang Y, Yenush L, Burks D, Myers MG Jr, Glasheen E, Copeland NG, Jenkins NA, et al. The *IRS2* gene on murine chromosome 8 encodes a unique signaling adapter for insulin and cytokine action. Mol Endocrinol. 1997; 11:251–262. [PubMed: 9013772]
48. Gibson SL, Ma Z, Shaw LM. Divergent roles for IRS-1 and IRS-2 in breast cancer metastasis. Cell Cycle. 2007; 6:631–637. [PubMed: 17361103]
49. Huang SS, Leal SM, Chen CL, Liu IH, Huang JS. Cellular growth inhibition by TGF-β1 involves IRS proteins. FEBS Lett. 2004; 565:117–121. [PubMed: 15135063]
50. Senthil D, Choudhury GG, Abboud HE, Sonenberg N, Kasinath BS. Regulation of protein synthesis by IGF-I in proximal tubular epithelial cells. Am J Physiol Renal Physiol. 2002; 283:F1226–F1236. [PubMed: 12388420]
51. Nguyen TQ, Goldschmeding R. Bone morphogenetic protein-7 and connective tissue growth factor: novel targets for treatment of renal fibrosis? Pharm Res. 2008; 25:2416–2426. [PubMed: 18266088]

52. Walsh DW, Godson C, Brazil DP, Martin F. Extracellular BMP-antagonist regulation in development and disease: tied up in knots. Trends Cell Biol. 2010; 20:244–256. [PubMed: 20188563]

53. Zhang H, Schulz TJ, Espinoza DO, Huang TL, Emanuelli B, Kristiansen K, Tseng YH. Cross talk between insulin and bone morphogenetic protein signaling systems in brown adipogenesis. Mol Cell Biol. 2010; 30:4224–4233. [PubMed: 20584981]

54. Bernal D, Almind K, Yenush L, Ayoub M, Zhang Y, Rosshani L, Larsson C, Pedersen O, White MF. Insulin receptor substrate-2 amino acid polymorphisms are not associated with random type 2 diabetes among Caucasians. Diabetes. 1998; 47:976–979. [PubMed: 9604879]

55. Kalidas K, Wasson J, Glaser B, Meyer JM, Duprat LJ, White MF, Permutt MA. Mapping of the human insulin receptor substrate-2 gene, identification of a linked polymorphic marker and linkage analysis in families with type II diabetes: no evidence for a major susceptibility role. Diabetologia. 1998; 41:1389–1391. [PubMed: 9833949]

56. Bottomley WE, Soos MA, Adams C, Guran T, Howlett TA, Mackie A, Miell J, Monson JP, Temple R, Tenenbaum-Rakover Y, et al. IRS2 variants and syndromes of severe insulin resistance. Diabetologia. 2009; 52:1208–1211. [PubMed: 19377890]

57. Pezzolesi MG, Poznik GD, Skupien J, Smiles AM, Mychaleckyj JC, Rich SS, Warram JH, Krolewski AS. An intergenic region on chromosome 13q33.3 is associated with the susceptibility to kidney disease in type 1 and 2 diabetes. Kidney Int. 2011; 80:105–111. [PubMed: 21412220]

58. Wang SN, Lapage J, Hirschberg R. Loss of tubular bone morphogenetic protein-7 in diabetic nephropathy. J Am Soc Nephrol. 2001; 12:2392–2399. [PubMed: 11675415]

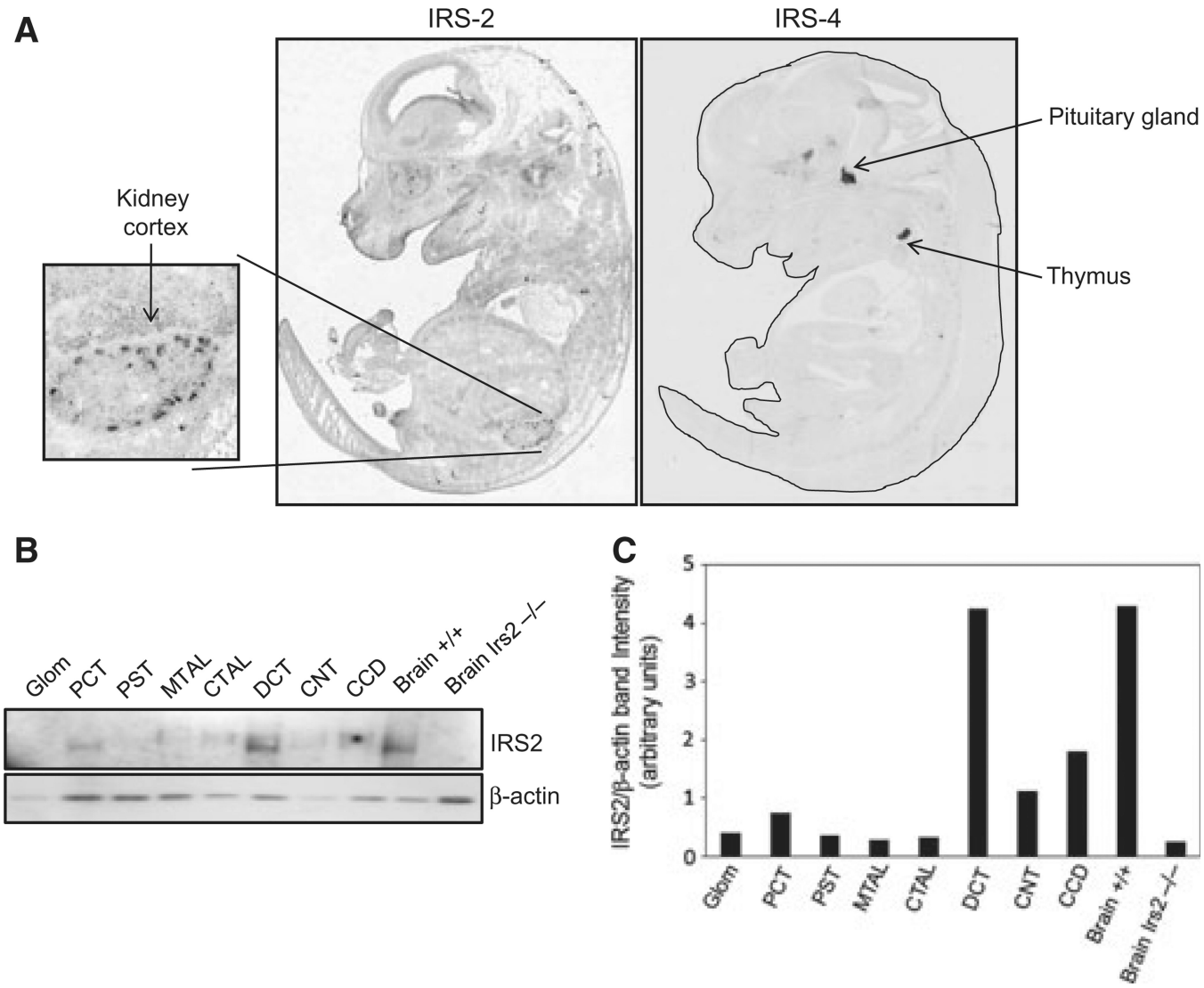

Fig. 1.

IRS2 is expressed in kidney tubular epithelium. (A) *In situ* hybridization of E14.5 mouse embryos stained for IRS2 and IRS4. IRS2 staining is evident in the kidney cortex (http://www.eurexpress.org/ee/). (B) Mouse kidneys were microdissected as described in Experimental procedures. Pools of 10–20 microdissected glomeruli (Glom), proximal convoluted tubule (PCT), proximal straight tubule (PST), medullary thick ascending limb (MTAL), cortical thick ascending limb (CTAL), distal convoluted tubule (DCT), cortical connecting tubule (CNT) and cortical collecting duct (CCD) were separated by SDS/PAGE and probed using antibody against IRS2. Brain extracts from wild-type and *Irs2*−/− mice were included as controls. β-actin was used as a loading control. Data are representative of four independent experiments. (C) Densitometry of IRS2 bands from kidney segments was performed using IMAGEJ. IRS2/β–actin intensity ratios were plotted for the indicated segments and for wild-type and *Irs2*−/− brain extracts.

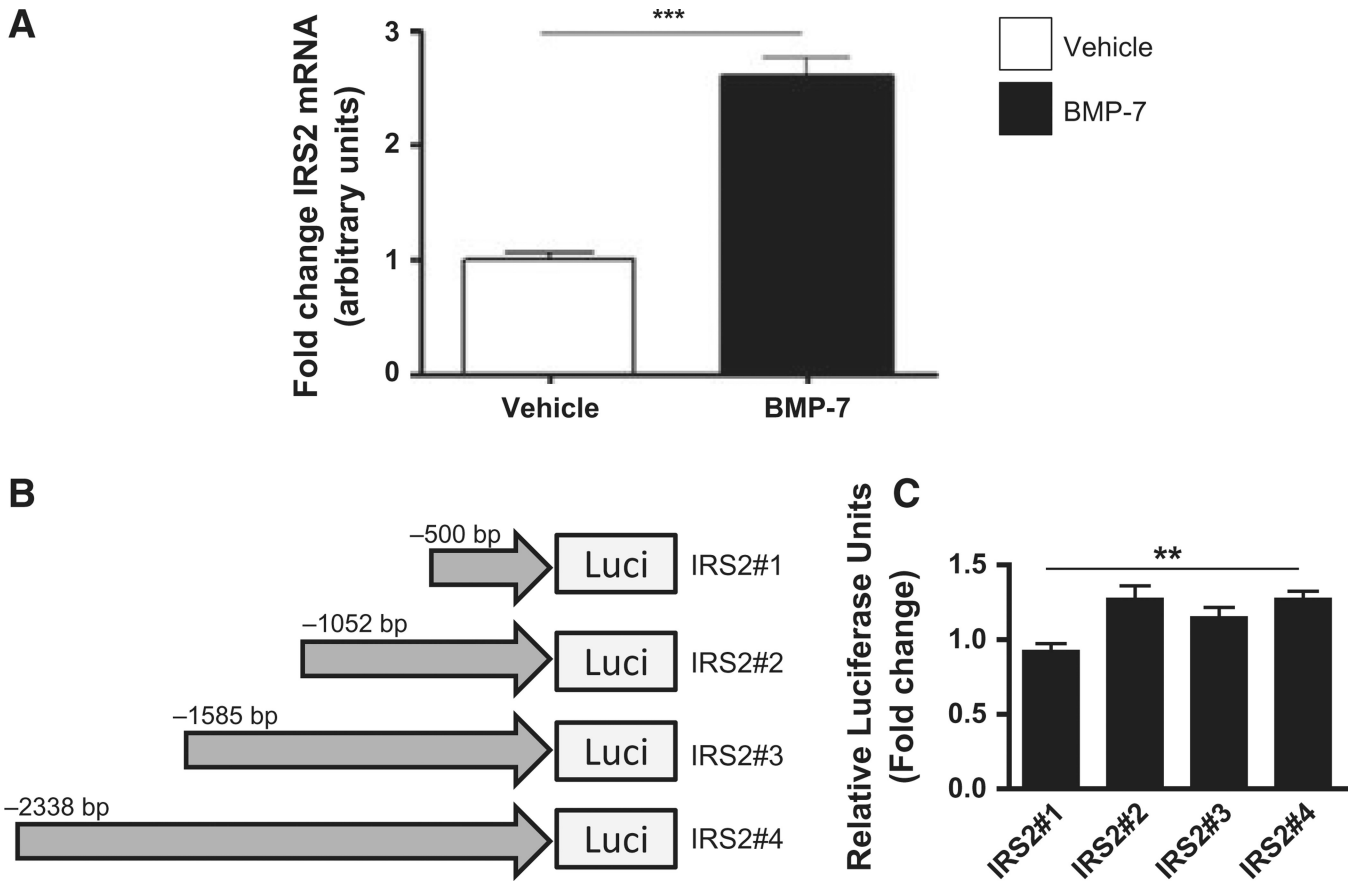

Fig. 2.

IRS2 gene expression is activated by BMP7. (A) HK-2 cells were starved of growth factors overnight and incubated with BMP7 (100 ng·mL^{-1}) for the indicated times. Total RNA was extracted and RT-PCR was performed using a TaqMan probe set specific for IRS2. Relative quantification values were obtained according to the $\Delta\Delta C_t$ method using 18S as a control, and normalized against control values (vehicle), which were set to 1 for each experiment. Experiments were performed three times in duplicate. Values are mean fold changes ± SEM, and significance was determined using Student's unpaired *t* test: ***$P < 0.001$. (B) Configuration of IRS2 promoter–luciferase constructs. Four constructs with increasing amounts of the predicted IRS2 promoter region (500, 1052, 1585 and 2388 bp) are shown. (C) HK-2 cells were transfected with the indicated IRS2 promoter–luciferase constructs cloned into the pGL3 plasmid (Promega, Southampton, UK). Cells were growth factor-restricted and treated with vehicle or BMP7 for 24 h. Extracts were prepared and assayed for luciferase activity as described in Experimental procedures. Experiments were performed three times in quadruplicate. Values are mean fold changes ± SEM. Statistical significance was determined using one-way ANOVA with Dunnett's *post hoc* multiple comparison test: **$P < 0.01$.

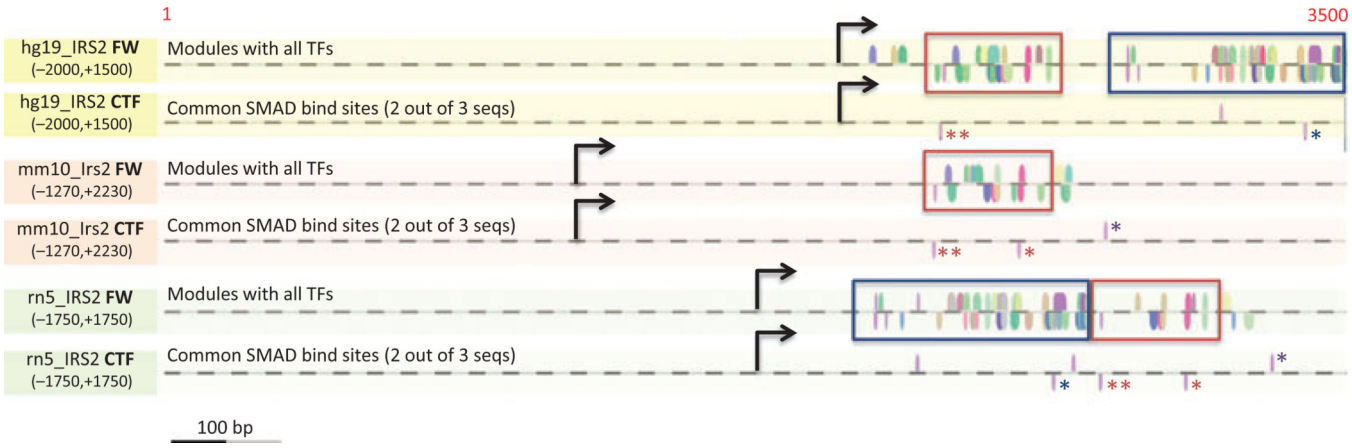

Fig. 3.

Predicted Smad4 transcription factor modules in the IRS2 proximal promoter regions. Genomatix FrameWorker (FW) and Common TFs (CTF) analyses (www.genomatix.de) were performed to search for predicted Smad4 binding sites (GCTCagac) in the indicated proximal regions of the human, mouse and rat IRS2 promoters. For each species, conserved transcription factor modules (coloured boxed regions identified by enrichment of two or three Smad site-containing FW models) are shown on the upper schematic, with the positions of the predicted Smad4 binding sites indicated on the lower line. Considering single Smad sites in this context also allowed us to tentatively distinguish among Smad sites conserved in all three of the promoters studied (**) or only in two of the promoters studied (*). The positions of the Smad4 binding sites are indicated on both the 5′ strand (above the line) and the 3′ strand (below the line). Note that the order of the two conserved modules of transcription factors is reversed in the rat IRS2 promoter compared to human. The position of the transcription start site is indicated by an arrow.

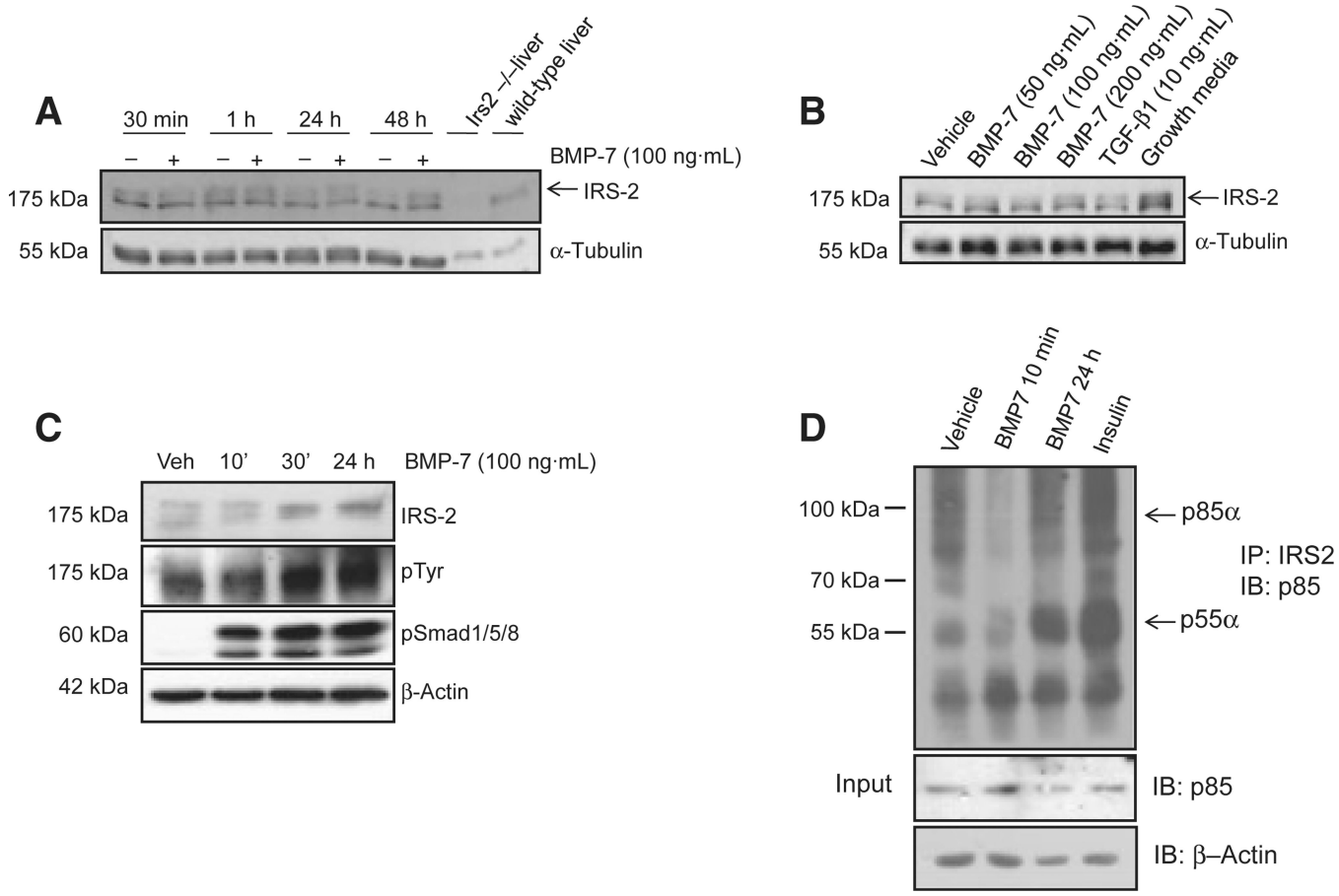

Fig. 4.

BMP7 increases tyrosine phosphorylation of IRS2 in HK-2 cells. (A) HK-2 cells were growth factor-restricted overnight and treated with vehicle (−) or 100 ng·mL^{-1} BMP7 (+) for the indicated times. Protein extracts were separated by SDS/PAGE and probed via Western blotting using antibodies against IRS2 (upper panel) or tubulin (lower panel). Wild-type and *Irs2*−/− mouse liver were included as controls. The position of IRS2 is indicated. The results are representative of $n = 4$ experiments performed in duplicate. (B) HK-2 cells were growth factor-restricted overnight and incubated with vehicle or increasing amounts of BMP7 as indicated for 24 h. Cells were also incubated with TGFβ1 (10 ng·mL^{-1}) and normal HK-2 growth medium as controls. Protein lysates were separated by SDS/PAGE and probed via Western blotting using antibodies against IRS2 or tubulin. The position of the IRS2 band is indicated. (C) HK-2 cells were growth factor-restricted overnight and incubated with vehicle or BMP7 (200 ng·mL^{-1}) for the indicated times. Protein lysates were used for IRS2 immunoprecipitation as described in Experimental procedures. Protein lysates were also probed for IRS2 expression, using phospho-Smad1/5/8 and β-actin antibodies as loading controls. The results are representative of $n = 4$ experiments performed in duplicate. (D) HK-2 cells were treated with vehicle or 100 ng·mL^{-1} BMP7 for the indicated times, or with insulin (100 nM) for 10 min. Protein lysates (250 μg) were incubated with antibody against IRS2 overnight, and immunoprecipitates were probed using antibody against p85α.

Protein lysates (‘input’) were also probed for p85α and β-actin. The positions of p85α and p55α are indicated.

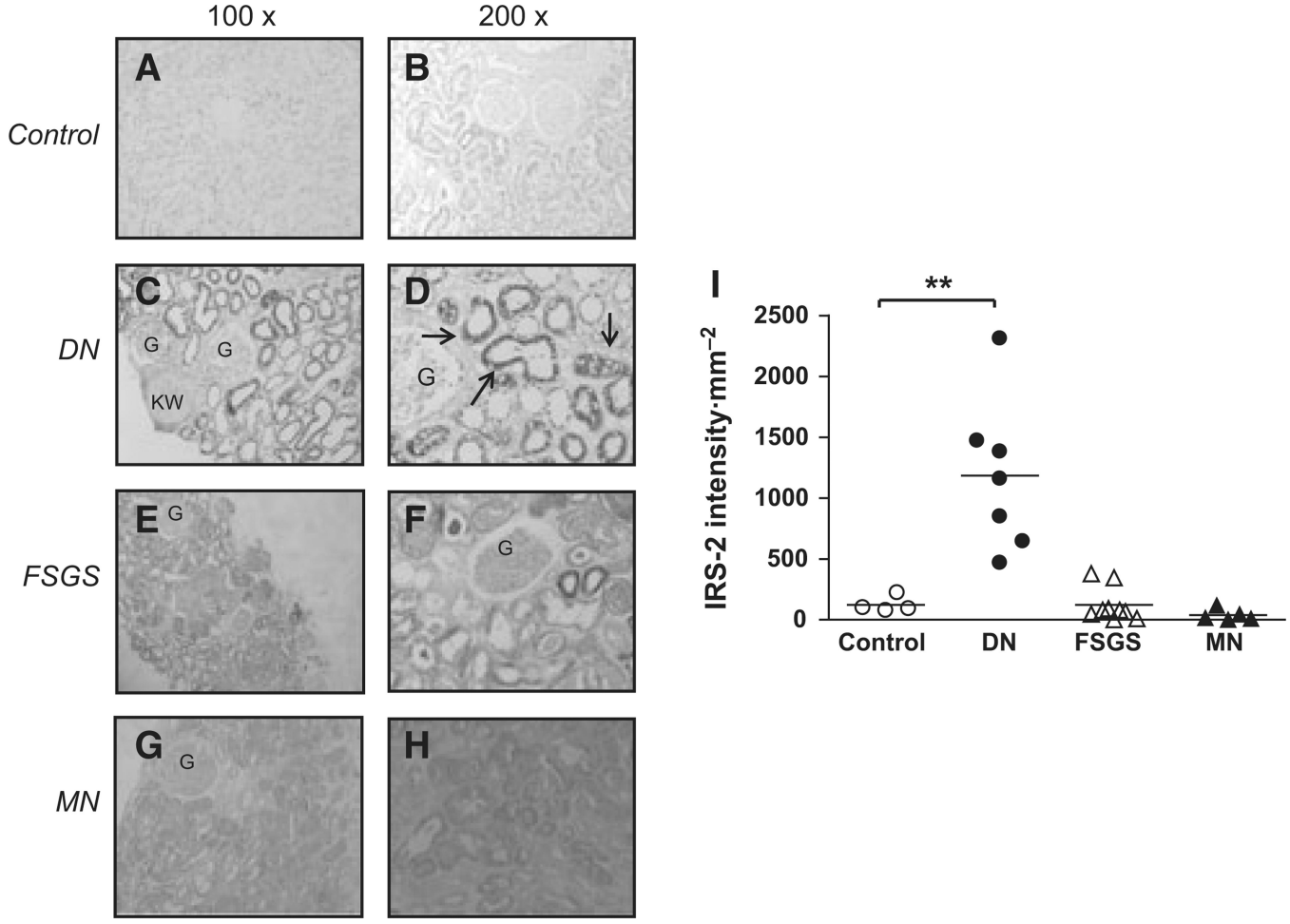

Fig. 5.

IRS2 is up-regulated in diabetic nephropathy. *In situ* hybridization images from a control patient (A, B), a diabetic nephropathy (DN) patient (C, D), a focal segmental glomerulosclerosis (FSGS) patient (E, F) and a membranous nephropathy (MN) patient (G, H) are shown. The position of glomeruli (G) and a Kimmelstiel–Wilson lesion (KW) are indicated. Strong IRS2 staining is evident in kidney tubules of DN patients (arrows). (I) IRS2 *in situ* hybridization intensity was scored by two independent observers as described in Experimental procedures. Values are median intensity/mm^2 ± SEM for control (n = 4), DN (n = 7), FSGS (n = 9) and MN (n = 3) patients. The data were compared using a Mann–Whitney non-parametric t test. Levels of IRS2 were significantly higher in DN patients versus control (**P < 0.01).

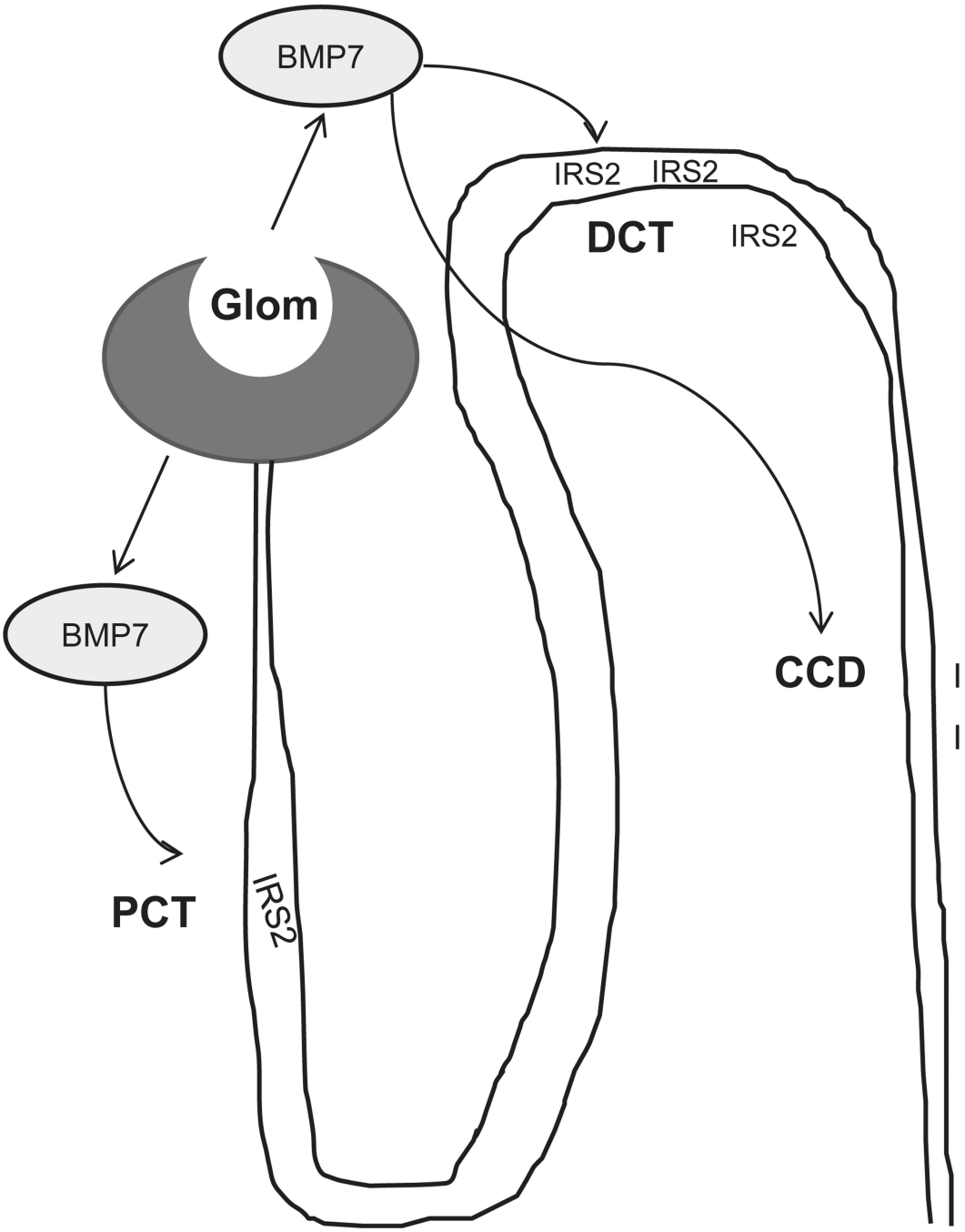

Fig. 6.

Schematic diagram summarizing BMP7-mediated regulation of IRS2 in distinct nephron segments. BMP7 released from the glomerulus activates IRS2 in the distal convoluted tubule (DCT) and cortical collecting duct (CCD), with lower levels of IRS2 expression present in the proximal convoluted tubule (PCT).

Table 1

Clinical correlates of control and diabetic nephropathy patients, with IRS2 *in situ* hybridization scoring. Renal biopsies from seven DN patients, nine FSGS patients, three MN patients and four controls were analysed. Control biopsies were obtained from polar nephrectomies of patients with kidney tumours. Estimated glomerular filtration rate was calculated using the modification of diet in renal disease method (www.mdrd.com). Chronic kidney disease (CKD) stage was defined based on Renal Association criteria (www.renal.org). The IRS2 *in situ* hybridization score is expressed as intensity/mm^2 tissue. DN, diabetic nephropathy; eGFR, estimated glomerular filtration rate; FSGS, focal segmental glomerulosclerosis; MN, membranous nephropathy.

Patient	Age	Sex	Proteinuria (g/24 h)	Creatinine (mg·dL^{-1})	Creatinine (μM) (mg·dL^{-1} × 88.4)	eGFR (ml/min/1.73 m^2)	CKD stage	IRS2 (intensity/mm^2)
DN1	51	M	2.8	2.6	229.8	26	4	645
DN2	50	F	9.9	1.2	106.1	48	3	468
DN3	52	F	13.9	2.5	221	20	4	848
DN4	65	F	3.1	1.3	114.9	41	3	1383
DN5	54	M	16	1.3	114.9	58	3	1472
DN6	63	F	10.5	3.3	291.7	14	5	2311
DN7	60	M	5	2.1	185.6	32	3	1160
FSGS1	25	F	36.7	2	176.8	32.3	3	79
FSGS2	20	M	9.5	1.45	128.1	65.9	2	346
FSGS3	28	F	6	0.64	56.5	117	1	380
FSGS4	54	M	2.3	1.75	154.7	43.4	3	10
FSGS5	52	F	2	1.25	110.5	47.8	3	47
FSGS6	58	M	7.5	1.6	141.4	47.4	3	79
FSGS7	11	F	11	0.69	60.9	> 90	1	66
FSGS8	18	M	2.6	0.5	44.2	> 90	1	0.6
FSGS9	10	M	4.7	0.58	51.2	> 90	1	16
MN1	12	F	5.1	0.56	49.5	> 90	1	16
MN2	60	F	2.1	1.81	160	30.3	3	118
MN3	26	F	0.8	0.8	70.7	> 90	1	10
Ctrl1	12	F	–	–	–	–	–	98
Ctrl2	52	M	–	–	–	–	–	221
Ctrl3	50	M	–	–	–	–	–	76
Ctrl4	38	M	–	–	–	–	–	91